

Probabilistic Inverse Analysis of Excavation-Induced Wall and Ground Responses for Assessing Damage Potential of Adjacent Buildings

Lei Wang · Zhe Luo · Junhua Xiao ·
C. Hsein Juang

Received: 2 February 2013 / Accepted: 3 November 2013 / Published online: 13 November 2013
© Springer Science+Business Media Dordrecht 2013

Abstract This paper presents an approach for the probabilistic inverse analysis of braced excavations based on the maximum likelihood formulation. Here, the soil parameters are updated using the observations of the maximum ground settlement and/or the maximum wall deflection measured in a staged excavation. The updated soil parameters are then used to refine the predicted wall and ground responses in the subsequent excavation stages, as well as to assess the building damage potential at the final excavation stage. Case study shows that the proposed approach is effective in improving the predictions of the excavation-induced wall and ground responses. More-accurate predictions of the wall and ground responses, in turn, lead to a more accurate assessment of the damage potential of buildings adjacent to the excavation. The proposed approach offers an effective means for a probabilistic inverse analysis of braced excavations.

Keywords Uncertainty · Probability · Inverse analysis · Building damage potential · Wall deflection · Ground settlement · Braced excavations

1 Introduction

The observational method (Peck 1969) is an important tool in geotechnical engineering. Peck recognized the importance of the observational method, as he “emphasized the need to first compute the various quantities that can be measured in the field and then close the gaps in knowledge on the basis of such measurements” (Wu 2011). In this paper, this observational method is applied to supported excavation. Here, field observations in a staged excavation are used to update soil parameters, which, in turn, are used to refine the predictions of the wall deflection, ground settlement and damage potential of buildings adjacent to the excavation in the subsequent stages of excavation.

The inverse analysis in the braced excavation is not uncommon. Conventionally, the finite element method (FEM) is utilized to predict the excavation-induced wall and ground responses (e.g., Hashash et al. 2004, 2006; Tang and Kung 2009, 2010). In the FEM analysis, the wall deflection, ground settlement and building damage potential are generally predicted and used to check against the acceptance criteria (i.e., Boone 1996). Due to the limited field explorations and laboratory tests, the soil parameters

L. Wang (✉) · Z. Luo · C. H. Juang
Glenn Department of Civil Engineering,
Clemson University, Clemson, SC 29634, USA
e-mail: lwang6@clemson.edu

J. Xiao
School of Transportation Science and Engineering,
Nanjing University of Technology, Nanjing 210009,
Jiangsu, China

C. H. Juang
National Central University, Jhongli, Taoyuan County
32001, Taiwan

used in the FEM analysis may not be representative of field behavior and thus the predicted excavation-induced responses often do not match the field observations. In a project such as braced excavation, the observed wall deflection and ground settlement from the initial excavation stages can be used to update the design soil parameters. The updated soil parameters, which represent the “refined” knowledge of the soil parameters at a given stage, can be used to refine the predictions in the subsequent excavation stages. As the excavation proceeds stage by stage, observations are collected in each stage and the soil parameters can be updated accordingly. Thus, the inverse analysis provides a means to update the prediction of ground responses and assessment of building damage during construction.

Conventional inverse analysis relies on the deterministic approach such as the least squares method, gradient method (Ou and Tang 1994), genetic algorithms (Levasseur et al. 2008), artificial neural networks (Hashash et al. 2006). It should be noted that the deterministic inverse analysis techniques could not deal with explicitly the uncertainty in the soil parameters. It is reported that the uncertainty in soil parameters has a significant influence on the predicted wall and ground responses in braced excavations (Hsiao et al. 2008). In this regard, it is desirable to conduct the probabilistic inverse analysis of a braced excavation. To this end, it is noted that several approaches, including the Kalman filter approach (Eykhoff 1974), the maximum likelihood method (Ledesma et al. 1996b), and the Bayesian method (Zhang et al. 2010b), have been shown effective for the probabilistic inverse analysis of some geotechnical problems.

Although FEM can be used in the probabilistic inverse analysis of braced excavations, it is more efficient, computationally, to combine the observational method with the empirical models such as KJHH (Kung et al. 2007) and KSJH (Schuster et al. 2009). These models, which were developed using well-documented case histories and finite element simulations, can be readily adopted to predict the excavation-induced wall and ground responses and the potential of building damage caused by these responses. To this end, the KJHH model is adopted in this paper for predicting the excavation-induced wall and ground responses in the probabilistic inverse analysis of braced excavations.

In this paper, the observational method is combined with the maximum likelihood formulation to update the soil parameters in braced excavations. The prior distributions of soil parameters are estimated based on those reported in the literature and engineering judgment. After the initial excavation stages are conducted, the maximum wall deflection and maximum ground settlement are measured (or observed). Those observations are used to update the soil parameters, and the updated soil parameters are presented as posterior distributions and characterized by their sample statistics. The updated soil parameters are then used to refine the predicted wall and ground responses in the subsequent excavation stages, as well as the building damage potential. This straightforward approach is repeated in a staged excavation, and the soil parameters are updated as the excavation proceeds. Comparing with the predictions using prior distributions, the predictions using the updated soil parameters generally result in an improved accuracy in the prediction of wall and ground responses, which in turn, yield an improved prediction of building damage potential.

2 Probabilistic Inverse Analysis Procedure

The inverse analysis of the wall and ground responses in a braced excavation requires three elements: (1) the observed data, (2) the model to prediction these data, and (3) the means for back analysis. In the present study, the observed data include the maximum wall deflection (δ_{hm}) and the maximum ground settlement (δ_{vm}). The model that is used to predict these data is KJHH model (Kung et al. 2007). This model is a semi-empirical model that was developed based on hundreds of simulations of case histories of excavations in clays using FEM. This model requires six input parameters, including the excavation depth H_e , the excavation width B , the system stiffness $S = EI/\gamma_w h_{avg}^4$, the normalized clay layer thickness ratio $\Sigma H_{clay}/H_{wall}$, the normalized undrained shear strength s_u/σ'_v , and the normalized initial modulus E_i/σ'_v . The reader is referred to Kung et al. (2007) for the detailed formulation of the KJHH model. It should be noted that as a simplified empirical method, the KJHH model cannot consider the effects of excavation sequence, construction methods, creep of soft soils

and retaining structures, and three-dimension excavation geometry. The probabilistic inverse analysis framework inherits this limitation of the KJHH model.

As reported in a reliability-based sensitivity study by Hsiao et al. (2008), two soil parameters (s_u/σ'_v and E_i/σ'_v) are found to be the main factors affecting the wall and ground responses of a braced excavation in clays. Therefore, the focus of this paper is to develop procedures for updating s_u/σ'_v and E_i/σ'_v in a braced excavation using the observed maximum wall and ground responses. Because of the uncertainties in these two soil parameters, the updating analysis (or inverse analysis) can be more effectively carried out using a probabilistic approach.

In the probabilistic inverse analysis, soil parameters s_u/σ'_v and E_i/σ'_v are treated as random variables, and all others are treated as constants. Furthermore, the model biases of the two component models (δ_{hm} and δ_{vm}) of KJHH model are considered in this inverse analysis. According to Kung et al. (2007), the model bias of the component model for δ_{hm} , denoted as c_h herein, has a mean value of 1.0 and a COV of 0.25; the model bias of the component model for δ_{vm} , denoted as c_v herein, has a mean value of 1.0 and a COV of 0.34. These model bias factors are assumed to follow normal distribution (Kung et al. 2007; Hsiao et al. 2008).

The third element of the probabilistic inverse analysis is the means for such analysis. In this study, the inverse analysis is implemented using the maximum likelihood principles. Here, the soil parameters are back calculated so that the likelihood of a hypothesis is maximized. The likelihood is proportional to the product of the prior distributions of input parameters and the probability density of the observed responses given input parameters (see “Appendix” section). Maximizing this likelihood is equivalent to minimizing the negative log-likelihood function, which is expressed as (Ledesma et al. 1996a; Wang et al. 2013):

$$S(\boldsymbol{\theta}) = (G(\boldsymbol{\theta}) - \mathbf{Y})^T \mathbf{C}_\varepsilon^{-1} (G(\boldsymbol{\theta}) - \mathbf{Y}) + (\boldsymbol{\theta} - \boldsymbol{\mu}_\theta)^T \times \mathbf{C}_\theta^{-1} (\boldsymbol{\theta} - \boldsymbol{\mu}_\theta) \tag{1}$$

where $\boldsymbol{\theta}$ is the vector of input parameters including s_u/σ'_v and E_i/σ'_v ; $G(\boldsymbol{\theta})$ is the predicted maximum wall deflections and maximum ground settlements based on input soil parameters $\boldsymbol{\theta}$; \mathbf{C}_ε is the covariance of

residual error vector; $\boldsymbol{\mu}_\theta$ is the prior mean vector of input parameters; \mathbf{C}_θ is the prior covariance matrix of the input parameters.

Thus, the posterior mean $\boldsymbol{\mu}_{\theta|Y}$ is obtained by minimizing $S(\boldsymbol{\theta})$. Then, the covariance of the posterior distribution can be calculated as follows (Tarantola 2005):

$$\mathbf{C}_p = (\mathbf{H}^T \mathbf{C}_\varepsilon^{-1} \mathbf{H} + \mathbf{C}_\theta^{-1})^{-1} \tag{2}$$

where \mathbf{H} is defined as the partial derivative vector evaluated at the posterior mean $\boldsymbol{\mu}_{\theta|Y}$:

$$\mathbf{H} = \left[\frac{\partial G(\boldsymbol{\theta})}{\partial \boldsymbol{\theta}} \right]_{\boldsymbol{\theta}=\boldsymbol{\mu}_{\theta|Y}} \tag{3}$$

The posterior distributions of the soil parameters (s_u/σ'_v and E_i/σ'_v) are then used for predicting the wall and ground movements in the subsequent stages of excavation.

3 Case Study: TNEC Excavation Case

To demonstrate the maximum likelihood-based formulation for the probabilistic inverse analysis, a well-documented excavation case history, the Taipei National Enterprise Center (TNEC), is analyzed here. TNEC excavation site is located in the Taipei Basin, and the seven-staged excavation is mainly conducted in deposits of soft to medium clay. The well-documented field observations of ground surface settlement and wall deflection of TNEC case (Ou et al. 1998) is well suited for the validation of the proposed approach.

The TNEC excavation was carried out using the top-down construction method with a maximum depth of 19.7 m. A diaphragm wall with 35 m in depth and 0.9 m in thickness was used as the retaining wall. The details of excavation can be found in Ou et al. (1998). Figure 1 shows the excavation depths for seven stages and the corresponding soil profile. The site of TNEC is mainly a clay-dominated site (Kung et al. 2007). It should be noted that s_u/σ'_v and E_i/σ'_v of the two clay layers in Fig. 2 are approximately the same, and the maximum wall and ground responses in this excavation are mainly influenced by s_u/σ'_v and E_i/σ'_v of the clay layers. As aforementioned, the soil parameters of the clay layers (s_u/σ'_v and E_i/σ'_v) are the dominating

Fig. 1 Soil profile and excavation depths of TNEC (adapted from Kung et al. 2007)

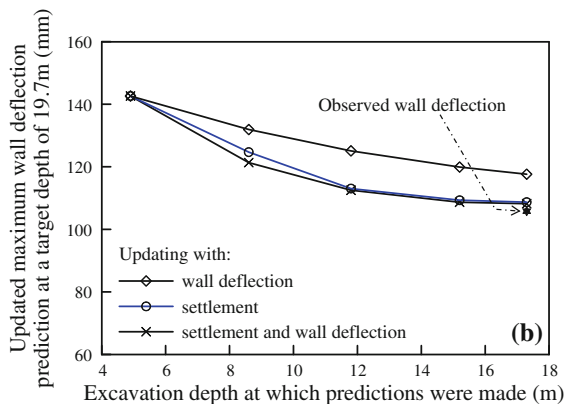
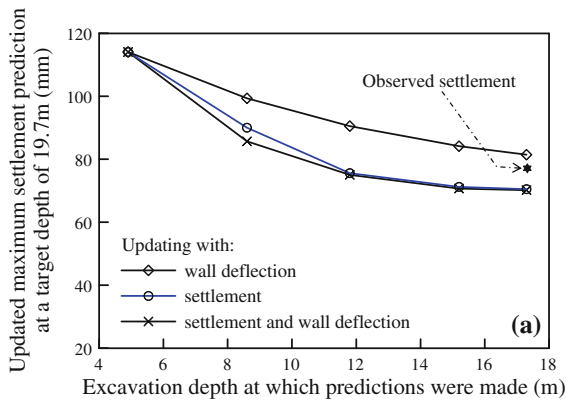
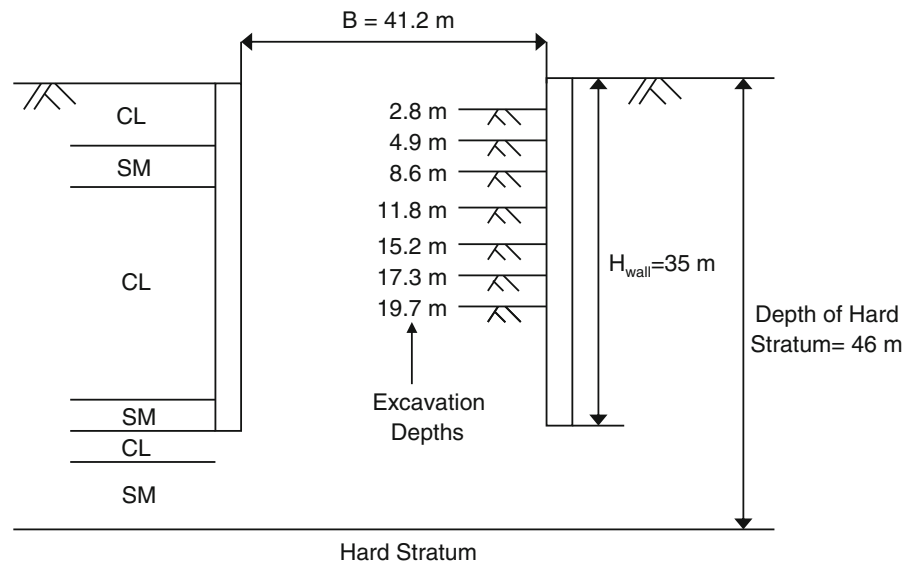


Fig. 2 Comparisons of updated predictions with three updating schemes (using Prior distribution 1)

parameters that will be updated with field observations. The input parameters of KJHH model of the TNEC case for each stage are listed in Table 1.

Table 1 Excavation depths and system stiffness of TNEC case history (adapted from Hsiao et al. 2008)

Factor	Excavation sequence (Stage No.)				
	3	4	5	6	7
Depth, H_e (m)	8.6	11.8	15.2	17.3	19.7
System stiffness, $EI/\gamma_w h_{avg}^4$	1,023	966	1,109	1,115	1,294

Other deterministic factors required for computing maximum wall deflection and ground surface settlement using KJHH model include: excavation width $B = 41.2$ m, normalized clay-layer thickness $\sum H_{clay}/H_{wall} = 0.87$

3.1 Updating Using Both Observed Wall Deflection and Ground Settlement

The prior distribution of the soil parameters must be estimated before the soil parameters can be updated. Based on the typical ranges of the two soil parameters s_u/σ'_v and E_i/σ'_v reported by Kung (2003), four different prior distributions of soil parameters are assumed and summarized in Table 2. For illustration purpose, Prior distribution 1 is adopted herein as the prior distribution of soil parameters vector (s_u/σ'_v and E_i/σ'_v). The parametric study using various assumed prior distributions will be presented later. Since there is no information regarding the correlation between two model bias factors, the correlation coefficient (ρ) is assumed to be zero for simplicity. Nevertheless, the effects of ρ on the updated results are investigated

Table 2 Statistics of four prior distributions used in the probabilistic back analysis process of TNEC case history (adapted from Juang et al. 2013)

Parameter	s_u/σ'_v		E_i/σ'_v	
	Mean	COV ^a	Mean	COV ^a
Prior distribution 1	0.25	0.16	500	0.16
Prior distribution 2	0.31	0.16	650	0.16
Prior distribution 3	0.27	0.16	550	0.16
Prior distribution 4	0.35	0.16	750	0.16

^a COV suggested by Hsiao et al. (2008) for Taipei clays. The effects of various assumed COVs are examined separately

later. It should be mentioned that the field observations from Stages 1 and 2 are not used in the updating process because the wall deformation shape at these early stages is of cantilever type, which is not compatible with the shape of bulging movement in latter stages (Kung et al. 2007). Thus, updating with the observations from Stages 1 and 2 is fruitless. Fortunately, the wall and ground responses in first two stages under normal workmanship are generally very small, and thus, the wall and ground movements at these early stages are negligible in the updating process (Hsiao et al. 2008; Juang et al. 2013).

As shown in Table 3, the predicted maximum ground settlement at excavation depth of 8.6 m (Stage 3) using the mean of soil parameters (Prior distribution 1) is 47.5 mm prior to Stage 3 of excavation, which is inconsistent with the observed settlement in field at excavation depth of 8.6 m (18.2 mm). After Stage 3 is completed, the soil parameters are updated using the observed wall and ground responses and the developed procedure. With the updated soil parameters in Stage 3, the maximum wall and ground responses in subsequent stages are predicted and compared with field observations. With the updated soil parameters, the predicted responses match better with the observations as evidenced in Tables 3 and 4. After Stage 4 of excavation is completed, the observations (settlement and wall deflection) at both Stage 3 and Stage 4 are employed to update further the soil parameters as well as the predictions of the wall and ground responses in subsequent stages. This process continues until the stage prior to the final stage (Stage 7).

As shown in Tables 3 and 4, at the completion of Stage 6, the predicted wall deflection and ground settlement prior to the final stage agree well with the observations at the completion of final stage (Stage 7).

It is also observed that the predicted wall deflection matches the field observation better than the settlement does; this is consistent with findings by other previous investigators: the wall deflection is generally easier to predict accurately; the prediction of settlement is, however, more difficult (Finno 2007).

The final excavation stage (Stage 7 with a final excavation depth of 19.7 m) is considered the most critical in the serviceability assessment of adjacent buildings. As shown in Fig. 2 (see line with symbol “×” for updating with both ground settlement and wall deflection), the predicted wall deflection and ground settlement at the completion of the last stage of excavation is refined as the excavation proceeds. It indicates that as the soil parameters are updated with more and more quality observations, the predicted wall and ground responses can be significantly improved accordingly.

3.2 Updating Using Observed Wall Deflection or Ground Settlement

When the observation data is limited (for example, in many case histories, only the observed wall deflection is available), the proposed procedure can be easily adapted for updating of soil parameters with only one type of observation (either wall deflection or ground settlement). For demonstration purpose, Prior distribution 1 is selected as the prior distribution of soil parameters. The aforementioned procedure for updating soil parameters using the maximum likelihood formulation is repeated using the observed wall deflection (or ground settlement) alone. With the updated soil parameters at various excavation stages, the predicted wall and ground responses at the final excavation stage are also plotted in Fig. 2. The results show the proposed framework is also effective and efficient even when the soil parameters are updated with only one type of response observation (either maximum settlement or maximum wall deflection).

It is also useful to examine the distributions of the predicted wall and ground responses using the updated soil parameters. The probability distributions of the updated ground settlement and wall deflection predictions, prior to the last stage, using three updating schemes are shown in Fig. 3. The results show that the means of the updated predictions are quite consistent with the observations. The variation in the predicted wall and ground responses is the smallest when both

Table 3 Observed and predicted maximum settlement using Prior distribution 1

Excavation		Maximum settlement (mm)					
		Observation	Prediction				
Stage	Depth(m)		Prior to excavation	End of 3rd stage	End of 4th stage	End of 5th stage	End of 6th stage
3	8.6	18.2	47.5	–	–	–	–
4	11.8	34.0	73.2	53.5	–	–	–
5	15.2	51.5	94.3	70.2	61.4	–	–
6	17.3	63.4	105.6	79.1	69.3	65.4	–
7	19.7	78.0	114.1	85.7	75.0	70.7	70.2

Table 4 Observed and predicted maximum wall deflection using Prior distribution 1

Excavation		Maximum wall deflection (mm)					
		Observation	Prediction				
Stage	Depth(m)		Prior to excavation	End of 3rd stage	End of 4th stage	End of 5th stage	End of 6th stage
3	8.6	44.6	59.4	–	–	–	–
4	11.8	64.0	91.6	75.7	–	–	–
5	15.2	79.9	117.9	99.4	92.0	–	–
6	17.3	99.0	132.0	112.1	104.0	100.5	–
7	19.7	105.8	142.6	121.3	112.5	108.7	108.2

types of observations are used in the updating. In addition, the variation of the predicted wall and ground responses using only settlement observation is smaller than that using only wall deflection. This is mainly because the error vector of the observational model for ground settlement is smaller than that for wall deflection. It should be noted that in the traditional back analysis of braced excavations, which tries to match “the prediction” to be exact as “observation,” the predicted ground settlement and wall deflection are a constant. However, the geotechnical inverse analysis involves model uncertainty as well as the uncertainty of soil parameters. Due to those uncertainties, it is desirable to interpret the updated soil parameters as well as the predicted wall and ground responses as a random variable rather than a single fixed value. The developed maximum likelihood-based procedure for the probabilistic back analysis of soil parameters is shown effective for the braced excavation problem.

It should be noted that the data points (observed settlement and deflection) presented in Figs. 2 and 3 were measured near the midpoint of the length of the TNEC excavation. According to Ou et al. (2000) and Kung (2003), the instrumentation was set in the

representative section of the TNEC excavation to avoid the corner effect.

4 Further Sensitivity Analyses and Discussions

4.1 Effect of Prior Distribution on the Updating Results

The posterior distribution depends on both model and prior distribution. Due to the insufficient field investigations and potential disturbance in sampling, the estimation of the prior soil parameters could vary significantly. In this regard, it is necessary to investigate the effects of estimated or assumed prior distribution on the updating results. Thus, in addition to Prior distribution 1 (Table 2), three other prior distributions are assumed based on the test results of Taipei clay, as shown in Table 2. The four assumed prior distributions cover the possible variation for the two soil parameters (s_u/σ'_v and E_i/σ'_v) for the TNEC case. The COV of the four distributions is set to be 0.16 as suggested by Hsiao et al. (2008). The effects of the magnitude of COV will be examined later.

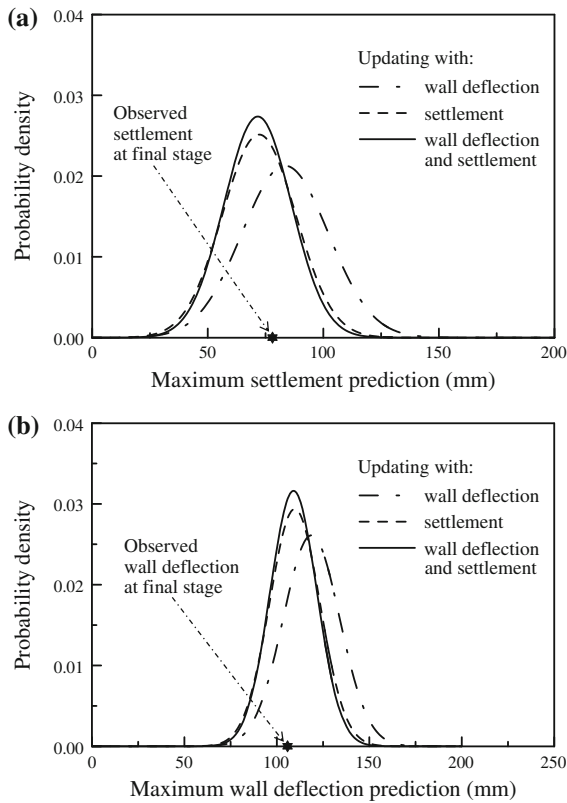


Fig. 3 Distributions of predictions prior to final stage of excavation (using Prior distribution 1)

The effects of prior distributions on the updated wall and ground responses are studied using two types of observations (both wall deflection and settlement). Following the aforementioned procedure, the updated mean values of s_u/σ'_v and E_i/σ'_v prior to various excavation depths are shown in Fig. 4. As shown in Fig. 4a, the updated mean values of s_u/σ'_v prior to last stage are almost identical no matter what prior distribution is assumed. The updated mean values of E_i/σ'_v also tend to converge as the excavation proceeds, regardless of the assumed prior distributions.

Figure 5 shows the updated COV for s_u/σ'_v and E_i/σ'_v with excavation depths. It is observed that the COV decreases as the excavation proceeds in this example. It indicates that the newly gained “information” from field observations can reduce the estimated variation of soil parameters. Although the variation of soil parameters is reduced most for Prior distribution

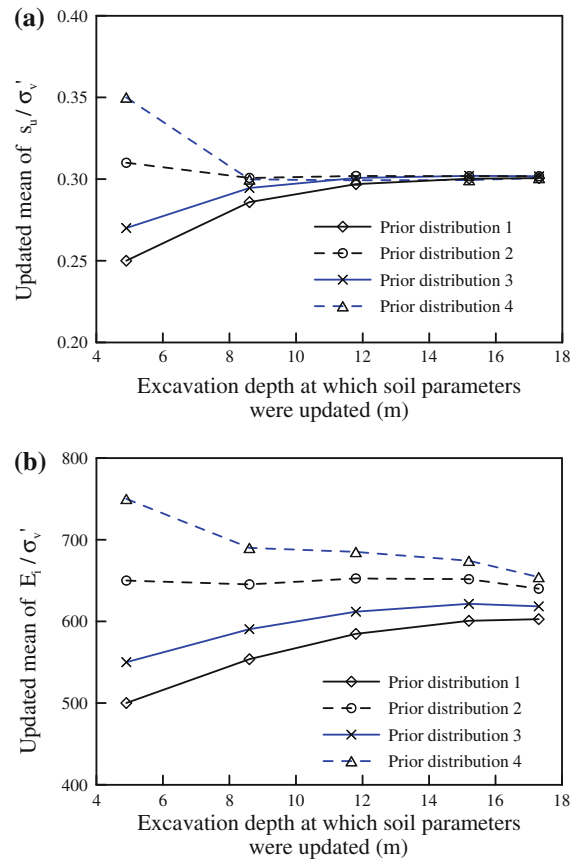


Fig. 4 Comparisons of updated mean of soil parameters prior to different stages with various prior distributions

1, the COV for all four assumed prior distributions decreases after updating, from 16 % to about 10 %.

The effect of different assumed COV on the updated results is plotted in Fig. 6. The distribution 1 is used for illustration and additional COV values of 0.10 and 0.30 are assumed to illustrate the possible overestimation and underestimation of the COV values for s_u/σ'_v and E_i/σ'_v . It can be found that the updated COV value of parameters decreases stage by stage with the updating process regardless which prior COV value is assumed. When the prior estimation of COV is at higher end (30 % in this example), the effect of reducing the parameter uncertainty is more effective, and the COV decreases to approximately 12 %. When the prior estimation of COV is already quite small (10 %), the COV can still be reduced (to approximately 6 % in this case).

The above results validate the efficiency of using observations to update the prior estimation of soil

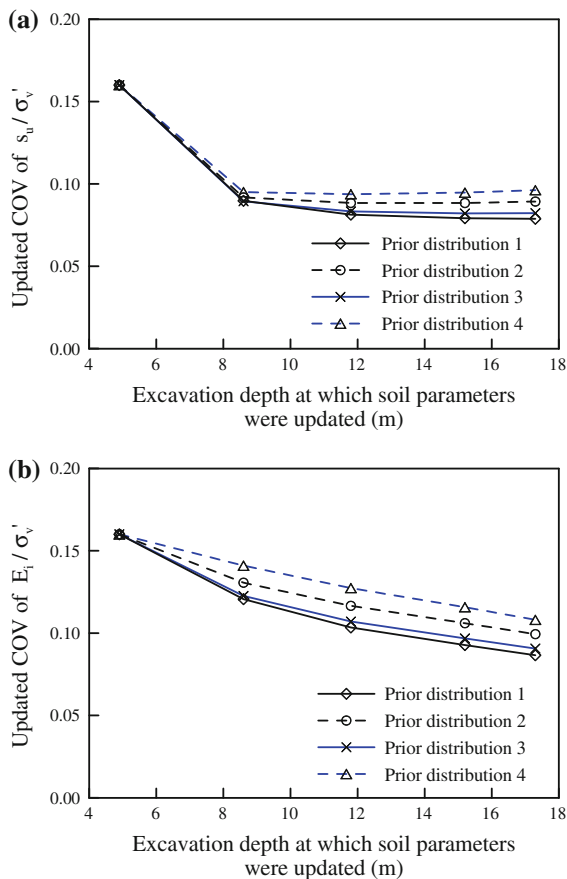


Fig. 5 Comparisons of updated COV of soil parameters prior to different stages with various prior distributions

parameters. Even if the prior estimation is not characterized perfectly initially, the observations during the excavation can “move” the prior estimation to its “true” value through the presented maximum likelihood procedure. Furthermore, with the reduced uncertainties in the input parameters, the uncertainty in the predicted ground and wall responses at the final stage of excavation is further reduced.

4.2 Effect of Correlation Between Bias Factors of KJHH Model

The effect of correlation between the bias factors of the two component models in KJHH model, namely wall deflection model and ground settlement model, is examined in this study. When no information regarding the correlation between the two component models is available, the two bias factors (c_b and c_v) may simply be assumed uncorrelated, as in the previous analysis

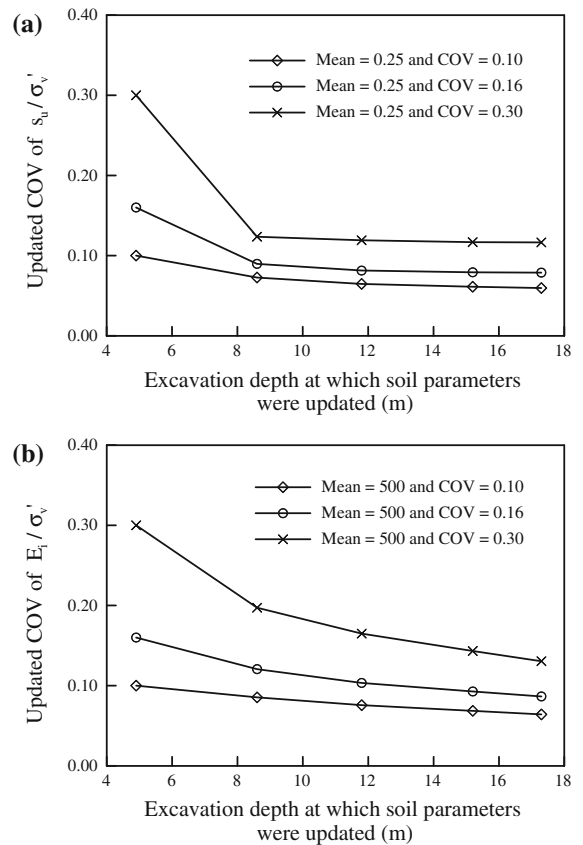


Fig. 6 Updated COV of soil parameters prior to different stages assuming various COV using Prior distribution 1

($\rho = 0$). However, the wall deflection and ground settlement in a braced excavation tend to be positively correlated, as reported by Kung et al. (2007).

To investigate the effect of the correlation between c_b and c_v , the aforementioned back analysis procedure is repeated using Prior distribution 1 with two positive correlation coefficient levels, $\rho = 0.5$ and 0.8 . The updated predictions for wall and ground responses with excavation depth at the three levels of correlation (0, 0.5, and 0.8) are shown in Fig. 7. The results show that the effect of the correlation between bias factors on the outcome of the developed updating procedure appears to be quite limited. Even with no correlation assumption, the developed procedure for updating soil parameters and predictions is still effective and yields no inferior outcome. Furthermore, this example demonstrates that the developed procedure for probabilistic inverse analysis can be easily adapted to incorporate the known correlation between the model biases of the component models.

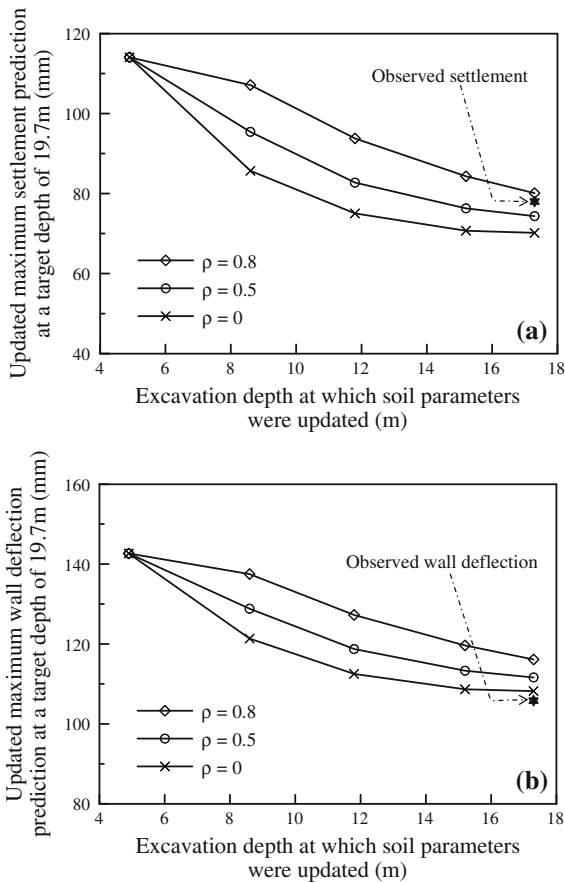


Fig. 7 Influence of correlation coefficient between model biases on updated predictions using prior distribution 1

5 Excavation-Induced Damage Potential of Adjacent Buildings

The excavation-induced wall and ground settlement can cause damage to adjacent buildings. Schuster et al. (2009) has developed a framework to evaluate the damage potential of buildings adjacent to the excavation. The basis for this framework is the predicted wall deflection and ground settlement. With the soil parameters being updated during the excavation using the field observations, the predictions of the wall and ground movements are updated. This follows that the prior assessment of building damage potential can be updated with the updated predictions of wall deflection and ground settlement. Thus, updating of the building damage potential is simply an extension of the developed updating scheme for wall and ground movement predictions.

The framework for excavation-induced building damage assessment established by Schuster et al. (2009) includes three components: (1) the profiles of the excavation-induced vertical and lateral ground movements using KJHH model (Kung et al. 2007) and KSJH model (Schuster et al. 2009), respectively; (2) computation of the angular distortion (β) and lateral strain (ϵ_l) using the empirical equations; and (3) determination of damage potential index (*DPI*) based on the calculated β and ϵ_l . The *DPI* is a normalization of the principal strain (Schuster et al. 2009):

$$DPI = 20 \times 10^3 (\epsilon_l \cos^2 \theta_{max} + \beta \sin \theta_{max} \cos \theta_{max}) \tag{4}$$

$$\tan(2\theta_{max}) = \beta / \epsilon_l \tag{5}$$

where β is angular distortion, ϵ_l is lateral strain, and θ_{max} is direction of crack formation measured from the vertical plane. The *DPI* value ranges between 0 and 100. A smaller *DPI* value indicates a lower damage potential.

In addition to the input parameters that are related to soil conditions (s_u / σ'_v and E_i / σ'_v) and other excavation parameters, the prediction of *DPI* for an adjacent building requires four additional data regarding the properties of the adjacent building. The first is the location of the building, characterized in terms of the distance from the excavation to the adjacent footings (e.g., d_1 and d_2 , as shown in Fig. 8, where d_1 represents the distance from the excavation to the nearest footing and d_2 represents the distance from the excavation to the furthest footing in a building). The second is the embedment depth of the building (D_1 in Fig. 8). The third is the soil-structure stiffness ratio, $(E_s L^2 / GHb)$, in which E_s is the soil stiffness in the region of footing influence, L is the length of building portion subjected to ground movement, G is the elastic shear modulus of the building, H is the height of the building, and b is the building wall thickness. The fourth is the structure cracking strain ϵ_r , which depends on characteristics of a specific building. It should be noted that in the *DPI* model, the existing building conditions are represented by two parameters including soil-structure stiffness ratio $(E_s L^2 / GHb)$ and structure cracking strain ϵ_r . These parameters, and thus the building damage potential, are of course affected by the structural types and building conditions (Schuster et al. 2009).

Detailed parameters for the properties of the adjacent buildings in TNEC case are documented in Schuster et al. (2009). Figure 8 shows the layout for Building D (Ou et al. 2000) that is adjacent to TNEC excavation. It should be noted that Building D could be split up into 4 bays for the purpose of computing *DPI* (Eq. 4). As reported by Schuster et al. (2009), Bay No. 4 is identified to be the critical bay (see Fig. 8) and thus it is selected here as an example to demonstrate the developed procedure for updating of *DPI*.

According to Schuster et al. (2009), the distances from the excavation to the nearest and furthest footings in Bay No. 4 (d_1 and d_2) are 25.5 and 31.0 m, respectively; the embedment depth of the footing (D_1) is 4 m; the soil-structure stiffness ratio ($E_s L^2 / GHb$) is estimated to be 15; the structure cracking strain ε_t is estimated to be 0.9. In this study, we follow the procedure by Schuster et al. (2009) to calculate *DPI*. The readers can refer to Schuster et al. (2009) for details.

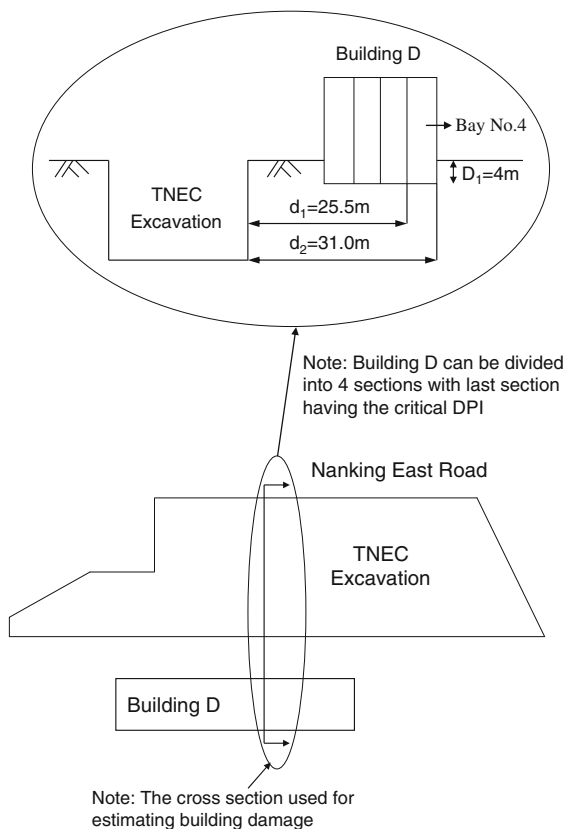


Fig. 8 Location of excavation and Building D in the TNEC case (adapted from Juang et al. 2011)

In this paper, the soil parameters are updated with the observed settlement and wall deflection. The updated soil parameters are then used to calculate the *DPI* at a target depth of 19.7 m (the final excavation stage). The four prior distributions of s_u / σ'_v and E_i / σ'_v , listed in Table 2 are adopted herein. Prior to Stage 3 (the excavation depth at this point is 4.9 m), the predictions of *DPI* for the final stage using the means of the four prior distributions are made and shown in Fig. 9. After Stage 3 excavation is completed, the observed maximum settlement and wall deflection are used to update the soil parameters. Then, the updated soil parameters are used to calculate *DPI* at a target excavation depth of 19.7 m (final excavation stage), and again, shown in Fig. 9 (the depth at which this prediction is made is 8.6 m). More and more observations are obtained as the excavation proceeds, and this updating procedure is repeated at excavation depths of 11.8, 15.2, and 17.3 m.

Figure 9 shows the predictions of the *DPI* at the target depth of 19.7 m (the final stage) using the updated soil parameters prior to Stages 3, 4, 5, 6, and 7 (the corresponding depths shown in Fig. 9 are 4.9, 8.6, 11.8, 15.2, and 17.3 m, respectively). As shown in Fig. 9, the predicted *DPI* values prior to Stage 3 of excavation differ significantly from each other, as the mean values of those prior distributions are different. With the updated soil parameters, the predictions of *DPI* tend to converge as shown in Fig. 9. Thus, the updating scheme presented in this paper is deemed effective for this evaluation of damage potential of an adjacent building. The predicted *DPI* values before the

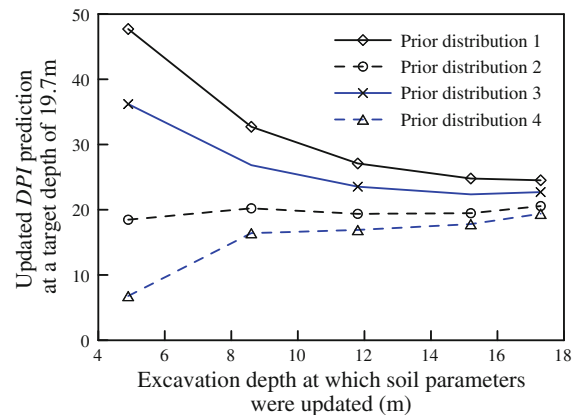


Fig. 9 Predicted *DPI* of Building D at the target excavation depth of 19.7 m with updated soil parameters under various assumptions of prior distribution

final stage of excavation (the excavation depth at this point is 17.3 m) converge into the range of 19–25 among the four prior distributions examined. According to the *DPI* criteria established by Schuster et al. (2009), the building with *DPI* = 19–25 would suffer a “slight damage.” As reported by Liao (1996) and Ou et al. (2000), the field observations during and after the construction showed that some cracks were found on the internal walls of Bay No. 4 of Building D in the TNEC excavation. This level of building damage would be characterized as “slight damage” according to the evaluation system established by Boscardin and Cording (1989). Thus, the updated prediction of *DPI* and the assessment of building damage are consistent with field observations.

In summary, the case study of TNEC for the wall and ground movements during excavation and their effect on an adjacent building shows that as the soil parameters are updated at each stage based on the observed settlement and wall deflection, the accuracy of the predicted wall and ground movements improves significantly. As a result of the improved predictions of wall and ground movements, the assessment of damage potential of the building adjacent to the excavation becomes more accurate.

6 Concluding Remarks

An approach for the probabilistic inverse analysis in braced excavations based on the maximum likelihood principle is presented. In this approach, the soil parameters (s_u/σ'_v and E_i/σ'_v) are updated with the observed wall and ground responses in a braced excavation. With the updated soil parameters, the predictions of those responses in the subsequent excavation stages and the predicted damage potential of an adjacent building are refined stage by stage. Comparing with the predictions using prior information, the predictions using the updated soil parameters are significantly improved in the case study of TNEC excavation.

Unlike the deterministic inverse analysis, the developed probabilistic inverse analysis approach allows for considerations of the variation in the soil parameters and model bias factors. Accordingly, the updated soil parameters are represented by the posterior distributions. The developed procedure is demonstrated to be effective regardless of the assumed prior distributions of the soil parameters provide that

such assumption is within the reasonable range. The efficiency and the effectiveness of this probabilistic analysis approach are illustrated through the case study of TNEC excavation in Taiwan.

Appendix: Formulation of Maximum Likelihood Method

The formulation of the maximum likelihood method for the probabilistic inverse analysis of braced excavations by Wang et al. (2013) is adapted in the current paper. The core component of this probabilistic inverse analysis framework is a simplified model, known as KJHH model (Kung et al. 2007), for predicting the excavation-induced wall and ground responses.

Symbolically, KJHH model can be expressed as:

$$\mathbf{y} = G(\boldsymbol{\theta}) \tag{6}$$

where $\boldsymbol{\theta}$ is the input vector including s_u/σ'_v and E_i/σ'_v ; \mathbf{y} is the response vector including both maximum wall deflection and maximum ground settlement at the end of a given excavation stage. The response of the excavation is related to the input parameter vector through the KJHH model denoted as G . The correlation between the vector of observations (\mathbf{Y}) and the vector of KJHH model predictions (\mathbf{y}) can be expressed as follows:

$$\mathbf{Y} = \mathbf{c} \cdot \mathbf{y} = \mathbf{c} \cdot G(\boldsymbol{\theta}) \tag{7}$$

where \mathbf{c} is a term that represents the model uncertainty. For illustration purpose, let us assume that only one pair of observations (i.e., one observed maximum ground settlement and one observed maximum wall deflection in the same excavation stage) is available for back analysis (or inverse analysis) of soil parameters. Note that the model uncertainty of the KJHH model is reflected through the use of bias factors in multiplication form (as in Eq. 7) with a mean vector of $\mu_{\mathbf{c}} = [\mu_{c_h}, \mu_{c_v}]$ and a covariance matrix of:

$$\sigma_{\mathbf{c}}^2 = \begin{bmatrix} \sigma_{c_h}^2 & \sigma_{c_{hv}}^2 \\ \sigma_{c_{vh}}^2 & \sigma_{c_v}^2 \end{bmatrix} \tag{8}$$

where $\sigma_{c_{hv}}^2 = \sigma_{c_{vh}}^2 = \rho \cdot \sigma_{c_h} \cdot \sigma_{c_v}$ and ρ is the correlation coefficient between two model bias factors c_h and c_v (Juang et al. 2013). In the common maximum likelihood formulation, the model bias of the observation model is often expressed in “addition” form

(Tarantola 2005). With the mean vector of model bias, $\mu_c = [1, 1]$, Eq. (7) can be converted into an addition form as follows (Wang et al. 2013):

$$\mathbf{Y} = \mathbf{c} \cdot G(\boldsymbol{\theta}) = \mu_c \cdot G(\boldsymbol{\theta}) + \varepsilon = \mu_c \cdot \mathbf{y} + \varepsilon = \mathbf{y} + \varepsilon \tag{9}$$

where ε is the residual error vector and is assumed to follow a multivariate normal distribution $\varepsilon \sim N(0, \mathbf{C}_\varepsilon)$. The covariance \mathbf{C}_ε depends on both the covariance of model bias factor vector σ_c and the input parameter vector $\boldsymbol{\theta}$, which can be expressed as:

$$\mathbf{C}_\varepsilon = \begin{bmatrix} (\sigma_{c_h} \cdot G_h(\boldsymbol{\theta}))^2 & (\sigma_{c_{hv}} \cdot G_{hv}(\boldsymbol{\theta}))^2 \\ (\sigma_{c_{vh}} \cdot G_{vh}(\boldsymbol{\theta}))^2 & (\sigma_{c_v} \cdot G_v(\boldsymbol{\theta}))^2 \end{bmatrix} \tag{10}$$

where $G_{hv}^2(\boldsymbol{\theta}) = G_{vh}^2(\boldsymbol{\theta}) = G_v(\boldsymbol{\theta}) \cdot G_h(\boldsymbol{\theta})$ and where $G_h(\boldsymbol{\theta})$ and $G_v(\boldsymbol{\theta})$ are the predicted δ_{hm} and the predicted δ_{vm} , respectively.

It should be noted that the aforementioned model uncertainty in the formulation of Eq. (10) is derived for the scenario when only one pair of observations (namely one maximum ground settlement and one maximum wall deflection) at a given excavation stage is adopted. If the observations from multiple excavation stages (say, n stages with totally $N = 2n$ observations) are available, the covariance \mathbf{C}_ε can be transformed into a $N \times N$ covariance matrix similar to one expressed in Eq. (10). For instance, when observations of the i th and the j th stages are available, \mathbf{C}_ε can be expanded into:

$$\mathbf{C}_\varepsilon = \begin{bmatrix} (\sigma_{c_h} \cdot G_{hi}(\boldsymbol{\theta}))^2 & (\sigma_{c_{hv}} \cdot G_{hvi}(\boldsymbol{\theta}))^2 & 0 & 0 \\ (\sigma_{c_{vh}} \cdot G_{vhi}(\boldsymbol{\theta}))^2 & (\sigma_{c_v} \cdot G_{vi}(\boldsymbol{\theta}))^2 & 0 & 0 \\ 0 & 0 & (\sigma_{c_h} \cdot G_{hj}(\boldsymbol{\theta}))^2 & (\sigma_{c_{hv}} \cdot G_{hvj}(\boldsymbol{\theta}))^2 \\ 0 & 0 & (\sigma_{c_{vh}} \cdot G_{vhj}(\boldsymbol{\theta}))^2 & (\sigma_{c_v} \cdot G_{vj}(\boldsymbol{\theta}))^2 \end{bmatrix} \tag{11}$$

where $G_{hi}(\boldsymbol{\theta})$ and $G_{vi}(\boldsymbol{\theta})$ denote the predicted maximum wall deflection and ground settlement at i th stage similar to Eq. (10). It should be noted that the correlation of model uncertainty exists only in the predicted wall deflection and ground settlement at the same stage, while observations at different stages are assumed independent from each other (Park et al. 2010).

Assuming that the soil parameters follow a multivariate normal distribution, with M input parameters, the probability density function can be expressed as (Ang and Tang 2007):

$$f(\boldsymbol{\theta}) = \frac{1}{\sqrt{(2\pi)^M |\mathbf{C}_\theta|}} \exp \left[-\frac{1}{2} (\boldsymbol{\theta} - \mu_\theta)^T \mathbf{C}_\theta^{-1} (\boldsymbol{\theta} - \mu_\theta) \right] \tag{12}$$

where μ_θ is the prior mean vector of input parameters and \mathbf{C}_θ is the prior covariance matrix of the input parameters.

As in Eq. (9), the residual error ε is assumed to follow a multivariate normal distribution with a zero mean and a covariance matrix of \mathbf{C}_ε . Thus, the probability density function of the observed responses (\mathbf{Y}), given input parameters $\boldsymbol{\theta}$, can be described as follows (Ledesma et al. 1996a; Zhang et al. 2010a):

$$f(\mathbf{Y}|\boldsymbol{\theta}) = \frac{1}{\sqrt{(2\pi)^N |\mathbf{C}_\varepsilon|}} \times \exp \left[-\frac{1}{2} (G(\boldsymbol{\theta}) - \mathbf{Y})^T \mathbf{C}_\varepsilon^{-1} (G(\boldsymbol{\theta}) - \mathbf{Y}) \right] \tag{13}$$

where N is the number of observations and \mathbf{C}_ε is $N \times N$ covariance matrix of model uncertainty. The likelihood is proportional to the product of the probability density of the observations (Eq. 13) and the prior

distribution (Eq. 12) as follows (Ledesma et al. 1996a):

$$L(\boldsymbol{\theta}) \propto f(\mathbf{Y}|\boldsymbol{\theta}) \cdot f(\boldsymbol{\theta}) \tag{14}$$

The posterior mean of $\boldsymbol{\theta}$, denoted as $\mu_{\theta|\mathbf{Y}}$, is an optimal value which maximizes Eq. (14). For computational efficiency, the logarithm of the likelihood function is selected as the objective function.

Thus, maximizing the likelihood (Eq. 14) is equivalent to minimizing the negative log-likelihood function, defined as $S(\theta) = -2 \ln L(\theta)$. This new likelihood function $S(\theta)$ can be simplified into Eq. (1) by dropping the constant terms.

References

- Ang AHS, Tang WH (2007) Probability concepts in engineering: emphasis on applications to civil and environmental engineering, 2nd edn. Wiley, New York
- Boone SJ (1996) Ground-movement-related building damage. *J Geotech Eng* 122(11):886–896
- Boscardin MD, Cording EJ (1989) Building response to excavation-induced settlement. *J Geotech Eng* 115(1):1–21
- Eykhoff P (1974) System identification. Parameter and state estimation. Wiley, New York
- Finno RJ (2007) Use of monitoring data to update performance predictions of supported excavations. In: Theme lecture in the proceedings, FMGM, international symposium on field measurements in geomechanics, ASCE, Boston
- Hashash YMA, Jung S, Ghaboussi J (2004) Numerical implementation of a neural network based material model in finite element analysis. *Int J Numer Meth Eng* 59(7):989–1005
- Hashash YMA, Marulanda C, Ghaboussi J, Jung S (2006) Novel approach to integration of numerical modeling and field observations for deep excavations. *J Geotech Geoenviron Eng* 132(8):1019–1031
- Hsiao ECL, Schuster M, Juang CH, Kung GTC (2008) Reliability analysis of excavation-induced ground settlement for building serviceability evaluation. *J Geotech Geoenviron Eng* 134(10):1448–1458
- Juang CH, Schuster M, Ou CY, Phoon KK (2011) Fully-probabilistic framework for evaluating excavation-induced building damage potential. *J Geotech Geoenviron Eng* 137(2):130–139
- Juang CH, Luo Z, Atamturktur S, Huang H (2013) Bayesian updating of soil parameters for braced excavations using field observations. *J Geotech Geoenviron Eng* 139(3):395–406
- Kung TC (2003) Surface settlement induced by excavation with consideration of small strain behavior of Taipei silty clay. Ph.D. thesis, Dept. of Construction Engineering, National Taiwan Univ. of Science and Technology, Taipei, Taiwan
- Kung GTC, Juang CH, Hsiao CL, Hashash Y (2007) Simplified model for wall deflection and ground surface settlement caused by braced excavation in clays. *J Geotech Geoenviron Eng* 133(6):731–747
- Ledesma A, Gens A, Alonso EE (1996a) Parameter and variance estimation in geotechnical back analysis using prior information. *Int J Numer Anal Meth Geomech* 20:119–141
- Ledesma A, Gens A, Alonso EE (1996b) Estimation of parameters in geotechnical back analysis—I. Maximum likelihood approach. *Comput Geotech* 18(1):1–27
- Levasseur S, Malécot Y, Boulon M, Flavigny E (2008) Soil parameter identification using a genetic algorithm. *Int J Numer Anal Meth Geomech* 32(2):189–213
- Liao JT (1996) Performance of a top down deep excavation. Ph.D. thesis, Dept. of Construction Engineering, National Taiwan Univ. of Science and Technology, Taipei, Taiwan
- Ou CY, Tang YG (1994) Soil parameter determination for deep excavation analysis by optimization. *J Chin Inst Eng* 17(5):671–688
- Ou CY, Liao JT, Lin HD (1998) Performance of diaphragm wall constructed using top-down method. *J Geotech Geoenviron Eng* 124(9):798–808
- Ou CY, Liao JT, Cheng WL (2000) Building response and ground movements induced by a deep excavation. *Geotechnique* 50(3):209–220
- Park JK, Gardoni P, Biscontin G (2010) Estimation of soil properties and deformation in staged constructions based on MCMC method. *Geotechnical Special Publication (GSP 199)*, pp 1885–1894
- Peck RB (1969) Advantages and limitations of the observational method in applied soil mechanics. *Geotechnique* 19(2):171–187
- Schuster M, Kung GTC, Juang CH, Hashash YMA (2009) Simplified model for evaluating damage potential of buildings adjacent to a braced excavation. *J Geotech Geoenviron Eng* 135(12):1823–1835
- Tang YG, Kung GTC (2009) Application of nonlinear optimization technique to back analyses of deep excavation. *Comput Geotech* 36(1–2):276–290
- Tang YG, Kung GTC (2010) Investigating the effect of soil models on deformations caused by braced excavations through an inverse-analysis technique. *Comput Geotech* 37(6):769–780
- Tarantola A (2005) Inverse problem theory and methods for model parameter estimation, 2nd edn. Elsevier Science, New York
- Wang L, Luo Z, Juang CH (2013) Updating uncertain soil parameters by maximum likelihood method for predicting maximum ground and wall movements in braced excavations. *Geotechnical Special Publication (GSP 229)*, pp 530–541
- Wu TH (2011) 2008 Peck lecture: the observational method: case history and models. *J Geotech Geoenviron Eng* 137(10):862–873
- Zhang J, Tang WH, Zhang LM (2010a) Efficient probabilistic back-analysis of slope stability model parameters. *J Geotech Geoenviron Eng* 136(1):99–109
- Zhang LL, Zhang J, Zhang LM, Tang WH (2010b) Back analysis of slope failure with Markov chain Monte Carlo simulation. *Comput Geotech* 37(7–8):905–912